



CHICAGO JOURNALS



The University of Chicago

---

Constructing Random Matrices to Represent Real Ecosystems

Author(s): Alex James, Michael J. Plank, Axel G. Rossberg, Jonathan Beecham, Mark Emmerson, Jonathan W. Pitchford

Source: *The American Naturalist*, Vol. 185, No. 5 (May 2015), pp. 680-692

Published by: [The University of Chicago Press](http://www.press.uchicago.edu) for [The American Society of Naturalists](http://www.asn.org)

Stable URL: <http://www.jstor.org/stable/10.1086/680496>

Accessed: 24/04/2015 04:39

---

Your use of the JSTOR archive indicates your acceptance of the Terms & Conditions of Use, available at <http://www.jstor.org/page/info/about/policies/terms.jsp>

JSTOR is a not-for-profit service that helps scholars, researchers, and students discover, use, and build upon a wide range of content in a trusted digital archive. We use information technology and tools to increase productivity and facilitate new forms of scholarship. For more information about JSTOR, please contact support@jstor.org.



*The University of Chicago Press, The American Society of Naturalists, The University of Chicago* are collaborating with JSTOR to digitize, preserve and extend access to *The American Naturalist*.

<http://www.jstor.org>

# Constructing Random Matrices to Represent Real Ecosystems

Alex James,<sup>1,\*</sup> Michael J. Plank,<sup>1</sup> Axel G. Rossberg,<sup>2,3</sup> Jonathan Beecham,<sup>2</sup> Mark Emmerson,<sup>3</sup> and Jonathan W. Pitchford<sup>4</sup>

1. Biomathematics Research Centre, University of Canterbury, Christchurch, New Zealand; and Te Pūnaha Matatini, New Zealand; 2. Centre for Environment, Fisheries and Aquaculture Science (Cefas), Lowestoft, United Kingdom; 3. School of Biological Sciences, Queens University Belfast, Belfast, United Kingdom; 4. Departments of Biology and Mathematics, University of York, York, United Kingdom

Submitted June 18, 2014; Accepted December 10, 2014; Electronically published March 11, 2015

Online enhancements: appendices.

**ABSTRACT:** Models of complex systems with  $n$  components typically have order  $n^2$  parameters because each component can potentially interact with every other. When it is impractical to measure these parameters, one may choose random parameter values and study the emergent statistical properties at the system level. Many influential results in theoretical ecology have been derived from two key assumptions: that species interact with random partners at random intensities and that intraspecific competition is comparable between species. Under these assumptions, community dynamics can be described by a community matrix that is often amenable to mathematical analysis. We combine empirical data with mathematical theory to show that both of these assumptions lead to results that must be interpreted with caution. We examine 21 empirically derived community matrices constructed using three established, independent methods. The empirically derived systems are more stable by orders of magnitude than results from random matrices. This consistent disparity is not explained by existing results on predator-prey interactions. We investigate the key properties of empirical community matrices that distinguish them from random matrices. We show that network topology is less important than the relationship between a species' trophic position within the food web and its interaction strengths. We identify key features of empirical networks that must be preserved if random matrix models are to capture the features of real ecosystems.

**Keywords:** community matrix, complexity, food web, interaction strength, stability, predator-prey interaction.

## Introduction

Interactions between species are central to the concept of an ecosystem. They are, however, both expensive and technically challenging to measure empirically. It is natural, therefore, that ecologists have sought to understand to what extent these interactions can be thought of as random and, furthermore, to understand and quantify the possible relationships between these interactions that best confer the

features of ecosystem stability, resilience, and dynamics observed in nature. For these reasons, theories involving randomly generated interactions between species have underpinned many influential ideas concerning the stability of complex ecological networks (May 1972; Pimm and Lawton 1978; Yodzis 1981; Bastolla et al. 2009; Allesina and Tang 2012).

May (1972) famously showed that, under certain assumptions, there is a limit to how “complex” a network ecosystem with a stable equilibrium can be. He then hypothesized that this was relevant to the stability of ecological networks. Stability, in this context, means that there is an equilibrium in which all species in the network survive at some positive density and that this equilibrium is robust to sufficiently small perturbations in the species densities. Under this definition, stability of the equilibrium is quantified by the leading eigenvalue of the Jacobian matrix evaluated at the equilibrium point, which describes the behavior of the system close to equilibrium. Whether complex ecosystems operate close to equilibrium is a matter of some debate, and local stability is not the only way of quantifying the resilience of an ecosystem to change (Grimm and Wissel 1997; McCann 2000). Other measures include, for example, permanence (Jansen 1987; Law and Blackford 1992), persistence (Bastolla et al. 2009; Thébault and Fontaine 2010; Gravel et al. 2011), and species-deletion stability (Pimm 1980). Nevertheless, local stability is a necessary condition for a persistent equilibrium and is a widely used measure of ecosystem robustness (Thébault and Fontaine 2010; Allesina and Tang 2012; Staniczenko et al. 2013), and we focus on local stability in this article.

The conclusions of May (1972) contradicted earlier ideas that ecosystems with more species—and more interactions among those species—are more likely to be stable (MacArthur 1955; Elton 1958). In reality, highly complex ecological networks—that is, networks with many species, many interactions, and strong interactions—do exist (O’Gorman and Emmerson 2010; Twomey et al. 2012), and empirical evidence frequently points to a positive relationship between

\* Corresponding author; e-mail: alex.james@canterbury.ac.nz.

Am. Nat. 2015. Vol. 185, pp. 680–692. © 2015 by The University of Chicago. 0003-0147/2015/18505-55562\$15.00. All rights reserved. DOI: 10.1086/680496

complexity and stability (Yodzis 1981; de Ruiter et al. 1995; McCann 2000; Gravel et al. 2011). Various theoretical explanations for this apparent “stability despite complexity” have been proposed, including a skew in the interaction strength distribution toward weak links (McCann et al. 1998; Emmerson and Yearsley 2004), weak links in long loops (Neutel et al. 2002), a pyramidal distribution of biomass across trophic levels (Neutel et al. 2007), the stabilizing effect of predator-prey interactions (de Angelis 1975; Allesina and Pascual 2008), and spatial colonization-extinction dynamics (Gravel et al. 2011). Interaction strengths are widely accepted to be very important, but the consequences for theoretical structure-stability relationships are not well understood.

Our aim is to explore the relative importance of some of these hypotheses for stability despite complexity and to investigate the consequences of two key assumptions we identify in random matrix models. To do this, we use 21 networks constructed from empirical data via three independent methods. A combination of numerical simulations, statistical analysis, and algebraic calculations is used to assess the important features of these empirically derived networks within the wider class of random models that aim to describe them.

The first assumption of May (1972) concerns the interactions between species. Species were assumed to interact with one another randomly, so that the architecture of the network—that is, which elements of the community matrix are nonzero—was described by an Erdős-Rényi random graph (Erdős and Rényi 1960). The strengths assigned to species interactions—that is, the weights of the nonzero network links—were normally distributed. To test the assumption of randomly generated interactions and intensities, we quantify the stability of the empirically derived food webs and compare it to the stability predicted by a random matrix. We use a suite of randomization algorithms with different assumptions about food web structure and interaction strength distributions. In almost all cases, we find that each empirically derived food web is substantially more stable than the corresponding randomized food webs. This shows that the assumptions built into the random matrices bias the results toward instability.

The second assumption concerns the intraspecific competition of each species. May (1972) assumed that all species had the same timescale for self-regulation at equilibrium, resulting in equal elements on the diagonal of the community matrix. We use simple dynamical systems analysis to show that normalizing the self-regulation terms in this way leads to a model that is not representative of real communities. In ecological terms, this requires a highly restrictive and untested assumption about trade-offs between species’ intrinsic growth rates and their interactions with other species. We investigate the consequences of this as-

sumption by exploring the effect on matrix stability of different methods for estimating the self-regulation terms. In contrast to the random-interactions assumption described above, the consequence of assuming equal self-regulation is a strong bias toward stability.

### Random Matrix Models

We assume that a given ecosystem comprises  $n$  species and that the population of each species is represented by its biomass density  $x_i$ , where  $i = 1, \dots, n$ . The dynamics of the system are then represented by a general system of differential equations,

$$\frac{d\mathbf{x}}{dt} = \mathbf{f}(\mathbf{x}), \quad (1)$$

where  $\mathbf{x} = (x_1, \dots, x_n)$  and  $\mathbf{f}$  is a function that depends on  $\mathbf{x}$ . We define the Jacobian matrix in its mathematical sense to mean the matrix describing the linearized dynamics at any given location (Wiggins 2003), that is,

$$J_{ij} = \frac{\partial f_i}{\partial x_j}. \quad (2)$$

When this matrix is evaluated at an equilibrium point of the system—that is, at a point  $\mathbf{x}^*$  such that  $\mathbf{f}(\mathbf{x}^*) = 0$ —it is referred to as a community matrix. This is closely related to but distinct from the matrix of coefficients of species interaction rates used to parameterize, for example, a Lotka-Volterra model (see “Random Matrices and Dynamic Models”). Local stability of an equilibrium is determined by the real part of the leading eigenvalue (i.e., the eigenvalue with the largest real part) of its associated community matrix: if that real part is negative, then the equilibrium is locally stable. Although stability is a binary on/off property, for stable equilibria we use the term “less stable” to mean farther from stability (i.e., having a leading eigenvalue with larger real part), and conversely for the term “more stable.”

May (1972) modeled ecological networks of  $S$  species using random  $S \times S$  community matrices,  $A$ . Each off-diagonal element  $a_{ij}$  of  $A$  is set to 0 with probability  $1 - C$  and drawn from a distribution with mean 0 and variance  $\sigma^2$  with probability  $C$ . The element  $a_{ij}$  represents the effect that a unit of species  $j$  has on the rate of increase of species  $i$  at equilibrium: if  $a_{ij}$  is 0, species  $j$  has no direct effect on species  $i$ . The parameter  $C$  is referred to as the connectance. May’s critical insight was to use Wigner’s semicircle theorem and the circular law of Metha (1967) to show that the real parts of the eigenvalues of this random matrix must all be less than

$$d_0 = \sigma\sqrt{SC}. \quad (3)$$

The variable  $d_0$  is commonly referred to as “complexity” and represents the relative strength of intraspecific com-

petition needed to stabilize a given food web. If the diagonal elements  $a_{ii}$ , representing the effects of intraspecific competition, are all set to  $-d_0$ , then all of the eigenvalues of the community matrix will have negative real parts, and the equilibrium will be stable (see “Random Matrices and Dynamic Models”). A matrix with a high value of  $d_0$  requires strong intraspecific competition to stabilize it. May (1972) used equation (3) to conclude that high connectance (large  $C$ ), a large number of species (large  $S$ ), or strong interactions (high  $\sigma$ ) in food webs lead to instability.

These results were generalized by Allesina and Tang (2012) to community matrices with a more specific structure in the interaction terms  $a_{ij}$ . This included predator-prey systems in which interactions are beneficial to one species and detrimental to the other ( $a_{ij}$  and  $a_{ji}$  have opposite signs). Tang et al. (2014) extended the stability condition to account for pairwise correlation between  $a_{ij}$  and  $a_{ji}$ . They showed that, with high probability, the leading eigenvalue of the community matrix will have real part less than

$$d_0 = \sqrt{SV}(1 + \rho) - E, \quad (4)$$

where  $\rho$  is the correlation between  $a_{ij}$  and  $a_{ji}$  and  $E$  and  $V$  are the mean and variance, respectively, of the off-diagonal elements (including zeros). This result, with its revised definition of complexity, indicates that (under the assumptions of random network topology) the negative pairwise correlation ( $\rho < 0$ ) one might expect to find in a predator-prey system should be a stabilizing factor.

### The Relationship between Random Matrices and Real Food Webs

There are numerous methods of constructing a community matrix from data, many of which rely on body size data, allometric scaling relationships, bioenergetic models, and/or interaction strength data. Brose et al. (2006), Otto et al. (2007), and Woodward et al. (2005a) explored the consequences of some of these assumptions and highlighted their importance in determining stability. We use three independent, established approaches, each relying on different sets of assumptions, to construct community matrices from empirical data from 21 food webs with distinct topologies. These consist of (1) eight successional food webs and four soil food webs (Neutel et al. 2002) constructed using the biomass flux method of Moore et al. (1996), (2) six marine ecosystems modeled using Ecopath with Ecosim (EwE; Christensen and Pauly 1992), and (3) three freshwater/estuarine ecosystems constructed using the predator-prey mass ratio (PPMR) model of Emmerson and Raffaelli (2004). See appendix A (apps. A–C are available online) for

details. The soil and freshwater systems are all food webs consisting only of predator-prey interactions; the marine systems contain a mixture of interaction types.

We set the diagonal elements of each empirically derived matrix to 0 and calculate the real part  $l_0$  of the leading eigenvalue as a measure of how far that matrix is from stability (May 1972; Neutel et al. 2002; Allesina and Tang 2012). Figure 1A plots  $l_0$  against complexity as defined by equation (3). Complexity is inversely correlated with stability but only weakly, and it predicts stability within two orders of magnitude at best. Figure 1B repeats the plot using the modified stability condition incorporating pairwise correlation in equation (4) (Tang et al. 2014). The only matrices for which equation (4) provides a substantially better prediction are the food webs constructed with the PPMR model (circles), which result in a strong negative pairwise correlation (Emmerson and Raffaelli 2004). The construction methods used in the other networks (see app. A) result in much weaker pairwise correlation, and accounting for it using equation (4) has almost no effect.

Figure 1 raises an important question: given that complexity alone cannot usefully predict stability in these empirically derived networks, which other network properties can? We test the hypothesis that randomly generated community matrices capture the essential properties of a real food web by comparing suites of randomly generated matrices to the empirically derived matrices, where each suite is defined by a set of ecologically motivated rules. We seek algorithms capable of emulating key properties of the empirical networks.

For each empirically derived matrix, we generate suites of 200 random matrices for each of 12 randomization algorithms and calculate the value of  $l_0$  for each randomization. If a particular network property is fundamental to stability, then alterations to the network that preserve this property should only minimally affect stability. Figure 2 shows the results of this process for one empirically derived community matrix. Every randomized matrix has the same size and connectance as the empirically derived matrix. The vertical line shows the real part of the leading eigenvalue of the empirically derived matrix,  $l_0 = 0.1$ . The histograms show the distribution of  $l_0$  generated by 200 realizations of each randomization algorithm.

Figure 2A shows the distribution for the random matrix proposed by May (1972): the network topology is Erdős-Rényi, and the nonzero entries are drawn from a normal distribution with mean 0 and the same variance as in the original matrix. The difference is striking: in the random matrices, the strength of intraspecific competition needed to stabilize the food web,  $l_0$ , is between 100 and 10,000 times greater than in the original matrix. Figure 2B shows the distribution of  $l_0$  for a network as in figure 2A but with the same pairwise sign structure (i.e., the same number of

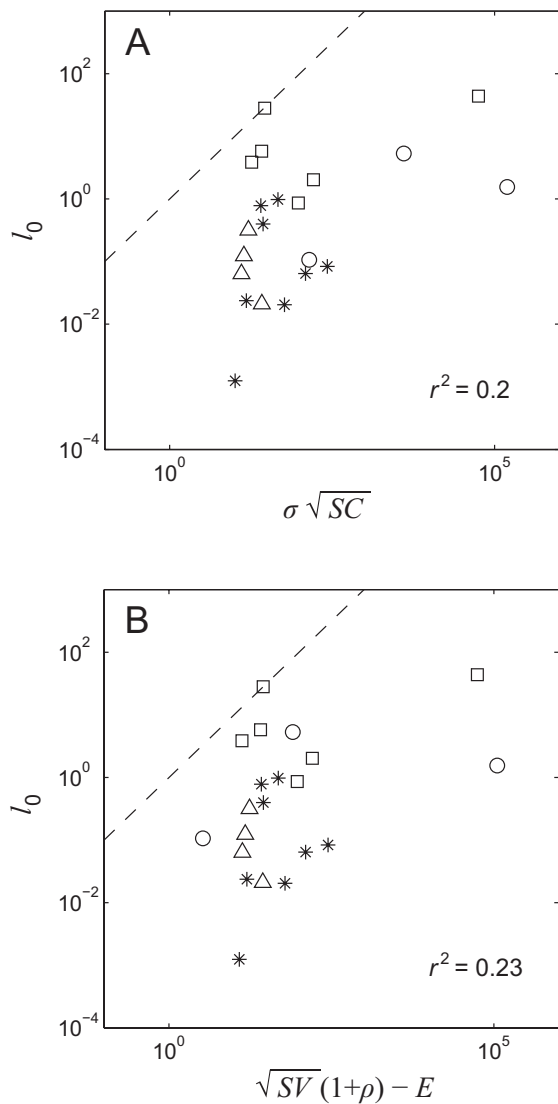


**Figure 1:** Stability-complexity relationship in 21 empirically derived food webs. The real part  $l_0$  of the leading eigenvalue against complexity  $d_0$  is defined by equation (3) (A) or (4) (B).  $S$  is the number of species;  $C$  is the connectance;  $\sigma^2$  is the variance of nonzero off-diagonal elements;  $E$  and  $V$  are the mean and variance, respectively, of all off-diagonal elements; and  $\rho$  is the correlation coefficient between  $a_{ij}$  and  $a_{ji}$  pairs. Diagonal elements are set to 0. The dashed lines show the line  $l_0 = d_0$ . Symbols indicate the method used to construct the community matrix: biomass flux = stars (successional webs) or triangles (soil webs); Ecopath with Ecosim = squares; predator-prey mass ratio = circles. Although complexity is correlated with stability, the relationship is weak and of little practical relevance. Many of the empirically derived networks are many orders of magnitude more stable than predicted by the criteria in equations (3) and (4).

predator-prey and competitive interactions) as the original matrix. These interaction pairs are randomly placed in the matrix, and the positive and negative elements are

randomly and independently generated from half-normal distributions with the same mean as in the original matrix. This approach is similar to that of Pimm and Lawton (1978) and Allesina and Tang (2012). This randomization still gives values of  $l_0$  approximately 100 times larger than in the original matrix. Figure 2C uses the same algorithm as figure 2B to generate the interaction strengths but preserves the empirical network topology rather than generating a topology at random. This is similar to an algorithm used by Jacquet et al. (2013). The difference in intraspecific interaction strength needed to stabilize the webs,  $l_0$ , between the randomizations and the empirically derived matrix is still large.

The preceding randomization algorithms all randomly generate nonzero elements of the community matrix from normal distributions and give values of  $l_0$  that are consistently more than 100 times greater than in the original matrix. Given this failure of randomly generated elements to capture the properties of the empirically derived matrices, we test a second category of algorithms that permute the actual matrix elements rather than randomly generating new elements. Figure 2E shows the distribution of  $l_0$  from an algorithm that moves existing pairs of interactions—that is, that destroys the topology of the original network—but holds  $(a_{ij}, a_{ji})$  pairs together and preserves pairwise correlation  $\rho$ . This algorithm gives a marked improvement over figure 2A–2C in retaining the original matrix properties: for this network, the value of  $l_0$  for the empirically derived matrix is now within the interquartile range of the distribution of  $l_0$  under the randomization. In figure 2F, pairs of elements  $(a_{ij}, a_{ji})$  are swapped with other existing pairs of elements, thus preserving the topology of the network. This additional constraint does very little to bring the stability of randomized matrices closer to that of the empirically derived matrices on which they are based. Finally, figure 2G applies a permutation of the positive elements and an independent permutation of the negative elements. This preserves the original topology and sign structure but destroys any pairwise correlation. Again, this modification gives very little change relative to algorithms E and F. Algorithms F and G are similar to those used by Yodzis (1981), de Ruiter et al. (1995), and Neutel et al. (2002).

Algorithms E–G, which use the original matrix elements rather than replacing them with random numbers, show a marked improvement in preserving the stability of the original matrix. This shows that the methods used to estimate the community matrices produce off-diagonal elements that yield relatively stable communities even if these elements are permuted and the topological structure of the original empirical networks is destroyed. The observation that there is little difference between E, F, and G shows that network topology (preserved in F and G) and pairwise correlation (preserved in E and F) are less important in

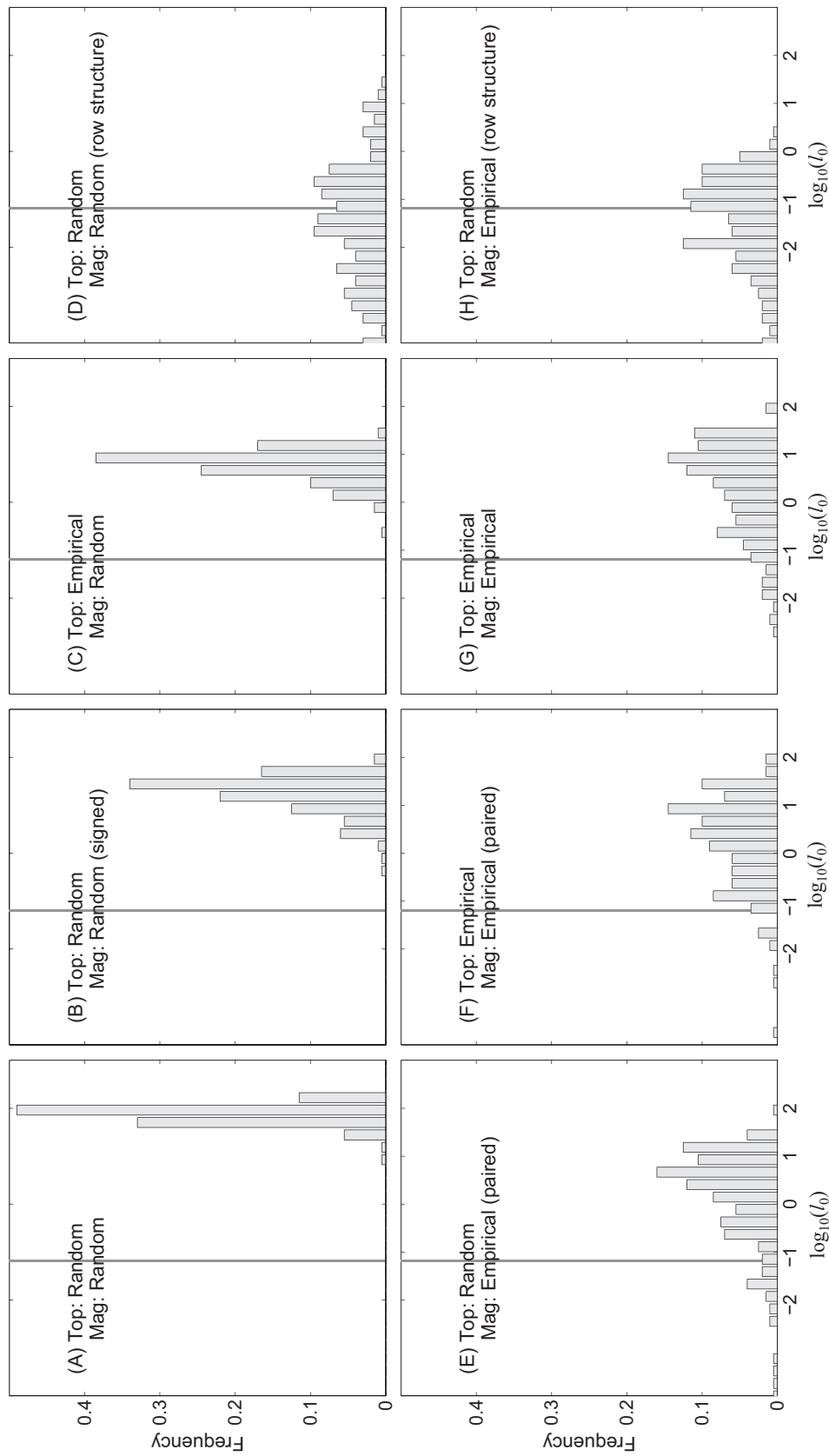


**Figure 2:** Randomized matrices are statistically many orders of magnitude less stable than the empirically derived matrix on which they are based. Graphs show the distribution of the strength of intraspecific competition needed to stabilize the web,  $l_0$  (the real part of the leading eigenvalue), for six different randomization algorithms, changing either or both of network topology (Top) and magnitude of interaction strengths (Mag), applied to an empirically derived community matrix (a successional soil food web). The vertical line shows the value of  $l_0$  for the empirically derived matrix. Randomizations that use a normal distribution to generate the nonzero elements (A–C) are orders of magnitude less stable than the empirically derived matrices; randomizations that move or swap the actual matrix elements (D–G) are closer but still show a consistent bias toward instability; randomizations that preserve row structure (D, H) better reflect the stability of the empirically derived matrices. See appendix B (available online) for details on the randomization algorithms.

this particular community than the distribution of matrix elements.

We repeated the above-described analysis using all 21 empirically derived community matrices (see app. A). We define the error for a random matrix to be  $\log_{10}(l_{\text{rand}}/l_{\text{emp}})$ , where  $l_{\text{rand}}$  and  $l_{\text{emp}}$  are the values of  $l_0$  in the randomized and empirically derived matrix, respectively. Figure 3 shows the mean and the 5th to 95th percentile range of the error for each randomization algorithm, applied to each of the 21 food webs. When these intervals exclude 0, the value of  $l_0$  for the empirically derived matrix lies in the tail of the distribution of  $l_0$  under the randomization scheme, showing that the scheme does not capture the relevant properties of the original matrix. The results in figure 3 confirm that the patterns seen in figure 2 for a single successional soil food web extend across a range of food webs. For the randomization algorithms that use normally distributed elements (A–C), the predictions are particularly biased, showing that the random matrices are much farther from stability than the empirically derived matrices. The distributions of  $l_0$  for these algorithms are relatively narrow, showing the similarity of all matrices generated by these algorithms. Importantly, all of the randomization algorithms tested are consistently biased toward instability (error > 0) for the majority of matrices.

As seen in figure 2, using the same distribution of elements (fig. 3E–3G) as in the empirically derived matrix helps to stabilize the randomized networks. Preserving either the empirical network topology (fig. 3F, 3G) or the pairwise correlation (fig. 3E, 3F) does not further improve the results for most networks. The notable exceptions to this are the food webs constructed with the PPMR model (circles), which have strong pairwise correlation and therefore respond well to algorithms that preserve this feature. This is consistent with the results of Tang et al. (2014), who also used the PPMR model in the construction methods.

The structure of predator-prey networks has been found to play an important role in stability (Levins 1979; Damacher et al. 2003; Allesina and Tang 2012). A pyramidal biomass pattern leads to strong row structure in community matrices: the variance of elements within a row is much less than the variance of elements between rows (Jacquet et al. 2013). This is borne out by the definition of an element of the community matrix:  $a_{ij}$  is the effect of a unit of species  $j$  on the rate of increase of species  $i$  at equilibrium. The rate of increase of species  $i$  is typically proportional to its abundance (see “Random Matrices and Dynamic Models”), meaning that the magnitude of elements in row  $i$  of the community matrix should be strongly correlated with the equilibrium abundance of species  $i$ .

To test the role played by row structure, we designed an algorithm that preserves the average magnitude of the elements in each row of the matrix. The positive/negative ele-

ments in each row are generated from normal distributions with the same means as in the original matrix (figs. 2D, 3D). To investigate the role played by interaction strength distribution in tandem with row structure, we designed a second algorithm that moves elements of the original matrix within rows in the lower triangle and moves the corresponding elements within columns in the upper triangle, holding pairs of elements ( $a_{ij}, a_{ji}$ ) together (figs. 2H, 3H; see app. B for details). Both of these algorithms destroy the original network topology but preserve stability remarkably well in most food webs. Using randomly generated elements (fig. 3D) destabilizes community matrices constructed by means of the PPMR model (circles) because it destroys the strong pairwise correlation in these matrices; the algorithm that preserves pairwise correlation (fig. 3H) preserves stability much better for these matrices. For the other food webs, there is little difference between fig. 3D and 3H, indicating that the row structure itself is more important than the precise distribution of interaction strengths.

Cycles of length three (interaction chains from species  $i$  to species  $j$  to species  $k$  and back to species  $i$ ), which typically arise from omnivorous interactions in food webs, can also affect stability. Neutel et al. (2002) showed that strong top-down effects in omnivorous relations tend to be spread across different cycles, meaning that the maximum cycle weight (where cycle weight is defined as the geometric mean of the strengths of the interactions in the cycle) tends to be lower in a real food web than in a randomized community matrix. Since cycle weights are closely linked to eigenvalues (Hofbauer and Sigmund 1998), they proposed that this helps make food webs stable. To test the role played by cycles in our empirically derived matrices, we designed simple algorithms that only change links that are not in a cycle of length three, either destroying or preserving the original network topology. Both algorithms preserve the number of cycles of length three, their weights, and the pairwise correlation of elements (see app. B for details). These are severe constraints: in most networks, only 25%–35% of links are changed by these algorithms. To enable a fair comparison with randomization algorithms that do not preserve cycles of length three, we devised corresponding algorithms that change the same number of links as the cycle-preserving algorithms but choose the links at random rather than because of their involvement in a cycle of length three. For the topology-changing algorithm (fig. 4A), there is little difference in the mean error between the algorithm that preserves cycles of length three and the algorithm that does not. For the topology-preserving algorithm (fig. 4B), preserving cycles of length three reduces error (see fig. B2 for the error distributions for each algorithm; figs. B1, B2, and C1 are available online). This shows that stability is promoted by the way in which cycles are positioned within the overall network topology (which is

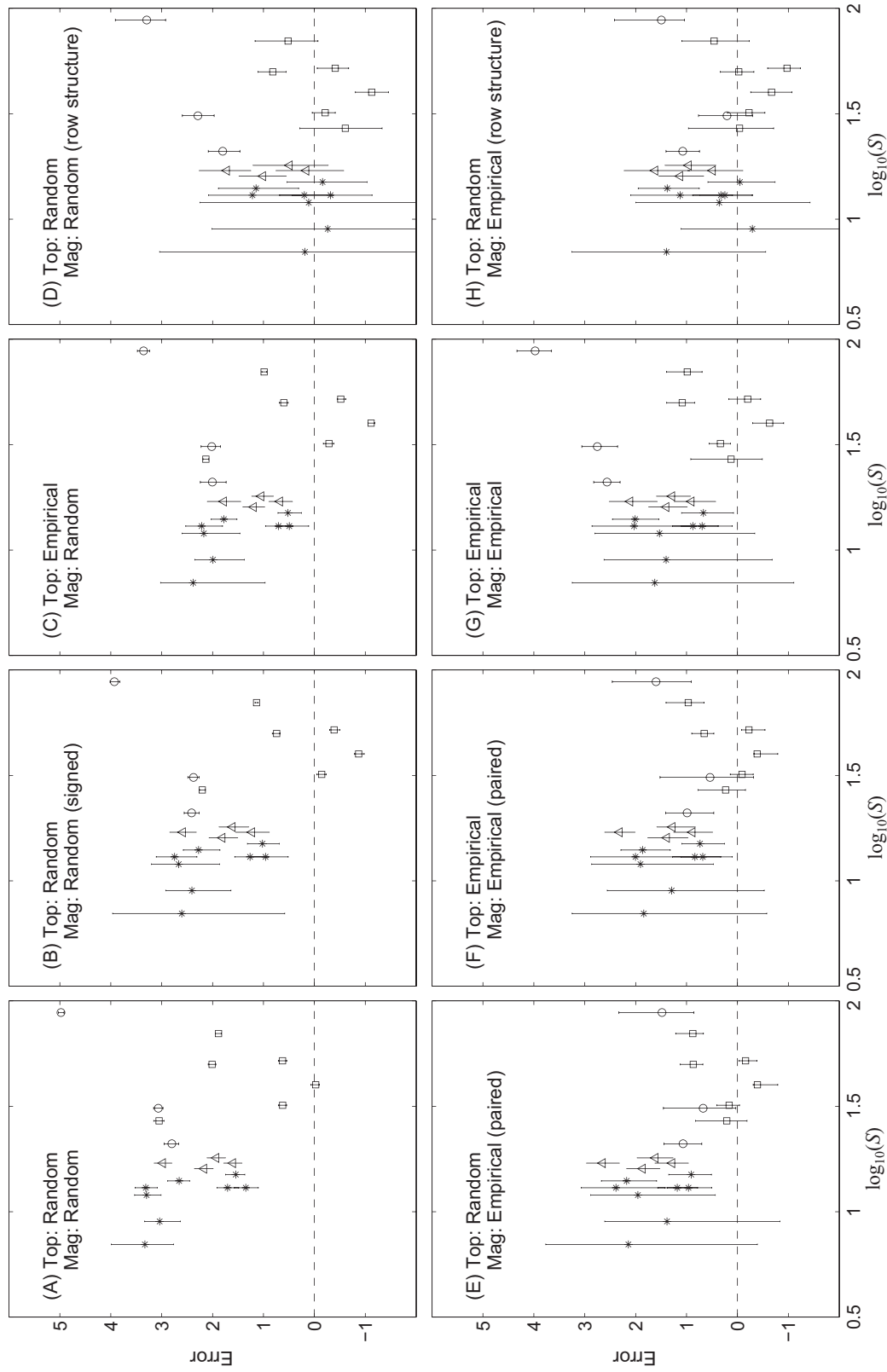


**Figure 3:** Differences in stability between empirically derived and randomized matrices across 21 communities and three construction methods. The distribution of error =  $\log_{10}(L_{\text{rand}}/L_{\text{emp}})$  for the same six randomization algorithms (A–H) is as in figure 2, changing either or both of network topology (Top) and magnitude of interaction strengths (Mag). The food webs are plotted against the number of species  $S$  in the web on the horizontal axis. See appendix B (available online) for details on the randomization algorithms. Symbols indicate the method used to construct the community matrix: biomass flux = stars (successional webs) or triangles (soil webs); Ecosim = squares; Ecopath-prey mass ratio = circles.



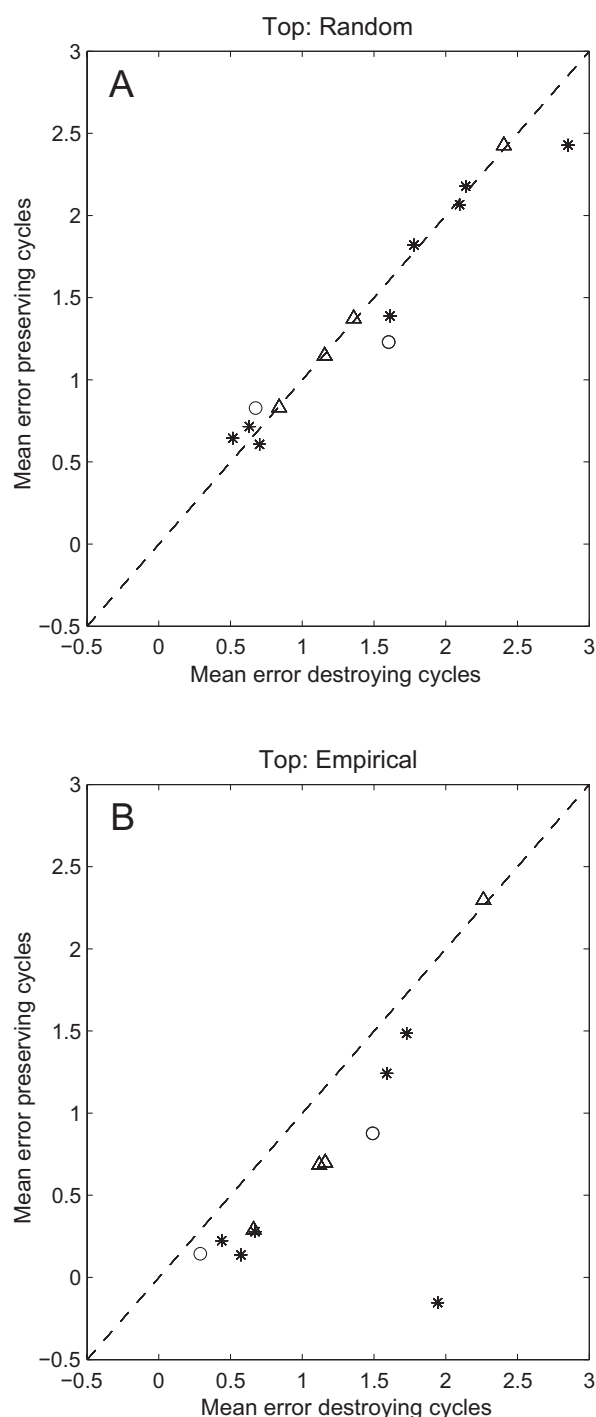


**Figure 4:** Stability is enhanced by the position of cycles within the overall network topology. The mean error =  $\log_{10}(l_{\text{rand}}/l_{\text{emp}})$  of randomization algorithms that preserve cycles of length three is plotted against the mean error of corresponding algorithms that change the same number of network links but do not preserve cycles. Randomizations in A and B destroy and preserve, respectively, the original network topology. See appendix B (available online) for details on the randomization algorithms. Symbols indicate the method used to

preserved only in fig. 4B) rather than simply by their weights (which are preserved in both fig. 4A and fig. 4B).

Of the randomization algorithms investigated, the cycle-preserving, topology-preserving algorithm (fig. 4B) is least biased but is highly restrictive, requiring information about the network topology, cycle structure, and distribution of matrix elements. In contrast, the algorithm shown in figure 3D requires only the means of the community matrix elements for each species and has purely random topology. This corresponds to May-type assumptions combined with realistic sign structure (Allesina and Tang 2012) and equilibrium biomasses for each species.

### Random Matrices and Dynamic Models

The results discussed in “The Relationship between Random Matrices and Real Food Webs” use the properties of general community matrices to indicate how stability may arise in complex networks. However, to truly understand the ecological implications of the results for random matrix models, it is helpful to consider a specific dynamic model rather than just a community matrix linearized around a hypothetical equilibrium point.

Most random matrix models, including those considered in “The Relationship between Random Matrices and Real Food Webs,” assume that all diagonal elements of the community matrix are the same, that is,  $a_{ii} = -d$  for some  $d > 0$ . This was justified by May (1972) with the statement “to set a time-scale, these damping times are all chosen to be unity” (i.e.,  $d = 1$ ). However, introducing the variability into the diagonal elements without changing their mean tends to increase the leading eigenvalue, and this effect cannot be removed by a rescaling of variables (Haydon 1994). Furthermore, the correspondence of diagonal elements with intraspecific effects is particular to simple generalized Lotka-Volterra models. More general models—for example, those with type 2 functional responses or other nonlinear interaction terms—do not have this property and generate diagonal elements that depend on interspecific interactions (de Angelis 1975; Haydon 1994). Therefore, some variation in the diagonal elements of the community matrix should be expected. The assumption of identical diagonal elements is crucial yet ecologically unjustified. In this section, we show that a dynamic model that is constrained to have equal diagonal elements in the community matrix behaves fundamentally differently from

---

construct the community matrix: biomass flux = stars (successional webs) or triangles (soil webs); predator-prey mass ratio = circles. Community matrices for which <90% of randomizations produce distinct matrices are not shown; this includes all of the Ecopath with Ecosim webs.

an unconstrained model and cannot exhibit one of the most common mechanisms for species loss.

Although the results of May (1972) did not rely on a specific dynamic model, the simplest model that generates a community matrix of the type considered by May (1972) and Allesina and Tang (2012) is a generalized Lotka-Volterra model,

$$\frac{dx_i}{dt} = x_i \left( r_i + \sum_{j=1}^S q_{ij} x_j \right), \quad (5)$$

where  $x_i$  is the biomass density of species  $i$ ,  $r_i$  is its intrinsic growth rate, and  $q_{ij}$  are referred to as Lotka-Volterra coefficients. This model assumes that species interactions can be described by “mass action” (type 1) terms. The coefficients  $q_{ij}$  correspond to the dynamic index measure of interaction strength *sensu* Berlow et al. (1999) and can be estimated empirically from predator-prey mesocosms (Emmerson and Raffaelli 2004). The diagonal element  $q_{ii}$  represents the strength of intraspecific competition, or self-limitation, for species  $i$  and must be nonpositive to prevent boundless growth of species  $i$  in isolation. Although equation (5) is the simplest model of an ecological network, the conclusions of this section extend to more general models (see app. C).

The community matrix for equation (5) has elements  $a_{ij} = q_{ij}x_i^*$ . This helps to explain the row weight patterns seen in the empirically derived matrices in “The Relationship between Random Matrices and Real Food Webs”: the elements in row  $i$  of the community matrix are proportional to the equilibrium biomass density  $x_i^*$  of species  $i$ . This emphasizes that the community matrix element does not represent the direct effect of species  $j$  on species  $i$  (which is  $q_{ij}$ ) and that  $a_{ii}$  does not represent the strength of intraspecific competition (which is  $q_{ii}$ ).

The system in equation (5) undergoes a transcritical bifurcation whenever one of the equilibrium abundances  $x_i^*$  becomes negative. During this transition, the abundance of species  $i$  gradually declines to 0, and the community moves smoothly to a different equilibrium in which species  $i$  is absent. Instability and species loss are thus associated with the gradual decline of one species to zero density.

At a transcritical bifurcation, the equilibrium abundance  $x_i^*$  for species  $i$  is 0, and so the diagonal element of the community matrix for species  $i$ ,  $a_{ii} = q_{ii}x_i^*$ , is also 0. Requiring all of the diagonal elements of the community matrix to equal  $-d < 0$  prevents this type of transition from occurring. It also imposes a constraint on the intrinsic growth rates  $r_i$  (see app. C):

$$r_i = d \sum_{j=1}^S \frac{q_{ij}}{q_{jj}}. \quad (6)$$

This constraint means that the equilibrium biomasses are  $x_i^* = -d/q_{ii}$ , which are always all positive since  $d > 0$  and  $q_{ii} < 0$ . Therefore, the only way in which a species can become extinct is via a degenerate bifurcation that makes the positive equilibrium become unstable, causing the system to move suddenly to a different equilibrium point (see app. C). Although sudden changes in community composition, such as regime shifts (Moellmann and Diekmann 2012), are certainly possible, a model that precludes species loss via gradual decline is unable to capture one of the simplest and most common mechanisms for change in ecological communities (Rossberg 2013). Hopf bifurcations, which lead to oscillatory dynamics, are also possible but are not directly associated with species loss.

Equation (6) can be interpreted as representing an ecological trade-off. A species that receives a net benefit from interactions with other species must compensate by having a negative intrinsic growth rate. For example, a top predator benefits from consuming prey ( $q_{ij} \geq 0$ ) but will die out in the absence of prey ( $r_i < 0$ ). Conversely, a species that is negatively impacted from interactions with other species (e.g., a basal resource or a species that competes with other species) must compensate by having a positive intrinsic growth rate. Although the idea that such trade-offs may operate in specific ecological circumstances is easy to argue, it is implausible that the intrinsic growth rates will be precisely tuned to satisfy equation (6). Any slight deviation from equation (6) results in a shift in model behavior, meaning that the assumption of equal diagonal elements makes the model structurally unstable.

Allesina and Tang (2012) argued that, in the limit as  $S \rightarrow \infty$ , variation among diagonal elements has a negligible effect on the leading eigenvalue compared with the effect of the off-diagonal elements. However,  $d_0$  scales as  $S^{1/2}$ . When scaling diagonal elements as  $S^{1/2}$  and keeping the coefficient of variation of the diagonal elements fixed, diagonal variance increases with network size. As a result, diagonal variance is not necessarily negligible for stability considerations, even as  $S \rightarrow \infty$ . To quantify the effect of variability in the diagonal elements of the 21 empirically derived community matrices, we added variability in one of two ways: first using randomly generated diagonal elements with the same variance as the off-diagonal elements, and second using the diagonal elements estimated from the empirical food web data. To enable a meaningful quantitative comparison with the zero-diagonal case, the diagonal elements were shifted so that their mean was 0.

We compared the real part of the leading eigenvalue of the matrix with diagonal variability to that of the matrix with diagonal elements set to 0 ( $l_0$ ; fig. 5). For all 21 food webs, using randomly generated diagonal elements (fig. 5A) gives a leading eigenvalue with substantially larger real part than using equal diagonal elements. Using the empirically

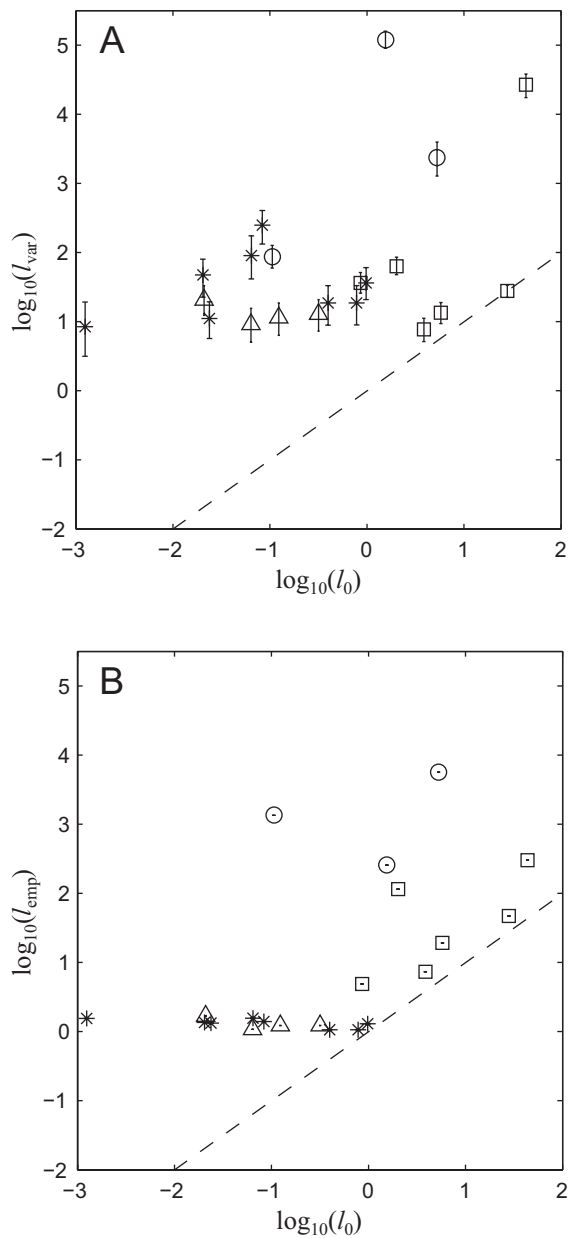


**Figure 5:** Adding variability to the diagonals of empirically derived community matrices decreases stability by orders of magnitude. The real part of the leading eigenvalue,  $l_0$ , of the matrix with diagonal elements is set to 0 against  $l_{\text{var}}$ , the real part of the leading eigenvalue of the matrix with randomly generated diagonal elements with the same variance as the off-diagonals (A); and  $l_{\text{emp}}$ , the real part of the leading eigenvalue of the matrix with empirically derived estimates for the diagonal elements (B). For each matrix with variable diagonal elements, a constant was added to all of the diagonal elements so that their sum was 0. Symbols indicate the method used to construct the community matrix: biomass flux = stars (successional webs) or triangles (soil webs); Ecopath with Ecosim = squares; predator-prey mass ratio = circles.

derived diagonal elements also gives a leading eigenvalue with larger real part in the majority of food webs (fig. 5B). For one of the three community matrix construction methods (used for the soil food webs; stars/triangles), the empirically derived diagonal elements dominate the matrix so strongly that all of the matrices have approximately the same leading eigenvalue when they are included. This shows that the standard assumption of equal diagonal elements consistently gives predictions that overestimate the stability of the equilibrium.

### Discussion

In the absence of detailed ecological data on species interactions, the use of random matrix models to make predictions about the relationship between ecosystem complexity and stability is widespread (Thébault and Fontaine 2010; Gravel et al. 2011; Allesina and Tang 2012). We have shown that using randomly generated network topology and interaction strengths can lead to predictions about local stability that differ by orders of magnitude from those of empirically derived models.

Various characteristics of real food webs—for example, the sign structure associated with predator-prey interactions (Allesina and Pascual 2008; Jacquet et al. 2013), the network topology (Haydon 2000; Tylanakis et al. 2010), and the distribution (McCann et al. 1998; Emmerson and Raffaelli 2004; Jacquet et al. 2013) and relative positioning (Yodzis 1981; de Ruiter et al. 1995; Neutel et al. 2002) of interaction strengths—have been suggested to have stabilizing influences. Our results show that including such characteristics in models can increase stability, but this is not always the case, even for larger networks where one would expect predictions based on random matrices to give the best results.

Measuring species interaction coefficients directly in complex food webs is impossible. The models themselves are necessarily simplifications of the real ecology, ignoring, for example, details of age and size structure. They may also amalgamate species into perceived functional groups, which reduces the apparent species richness. Further assumptions and simplifications are necessary to convert empirical data into estimated community matrices. One of the strengths of our study is that the empirical matrices originate from three independently established sets of modeling assumptions: the biomass flux model (Moore et al. 1996), EwE (Christensen and Pauly 1992), and the PPMR model (Emmerson and Raffaelli 2004). None of these approaches is “correct,” and each has arisen from ecological and data-driven constraints specific to the systems under study. Nevertheless, the resulting community matrices represent our best estimates of ecological reality. Where consistent patterns emerge from our analysis of empirical net-

works derived in different ways, this provides evidence that these ecosystems contain structure that is not captured by simple random matrix models.

Our study shows that network topology may be less important for community stability than widely thought. For example, Tylianakis et al. (2010) summarized the attributes of network topology thought to confer stability. Our results in figure 3C, 3F, and 3G show that it is possible to have two networks with identical topology but with key properties that vary by up to four orders of magnitude. Conversely, our results in figure 3D show that a random network topology with a particular organization of interaction strengths can come closer to empirical data. These results do not imply that topology has no effect, but they do show that it is less important than the distribution of interaction strengths.

We designed new randomization methods to quantify the role played by two important features of real ecological networks—namely, cycles of length three and row structure in the community matrix—in determining stability. We have shown that randomizations that preserve either of these properties better reflect the stability of the empirically derived network, although for cycles of length three the results are less marked than for row structure. That each of these properties involves a combination of network topology and the sizes of the community matrix elements emphasizes our finding that results based on randomizations that ignore or make unjustified assumptions about either of these features do not usefully reflect ecological reality.

Previous studies have focused on different properties of community matrices. Neutel et al. (2007) saw a correlation between cycle weights and stability in data from soil food webs; Jacquet et al. (2013) found that removing trophic structure in community matrices from EwE models adversely affected stability; and Tang et al. (2014) highlighted the role played by pairwise correlation in community matrices constructed using allometric scaling laws based on body mass (Brose et al. 2006; Reuman et al. 2009; Pawar et al. 2012). Our study unifies these seemingly disparate findings by including community matrices constructed using each of these three methods and showing that different factors are more important for stability in these different types of community. For instance, pairwise correlation is important in communities where it is strong, but other factors—most notably row structure—dominate in communities where it is weaker.

On the basis of empirical and theoretical considerations, Rossberg (2013) argued that transcritical bifurcations involving gradual decline of a species to zero density are the dominant form of loss of local stability in ecological communities. Community matrices where the diagonal elements are assumed to be equal prevent this type of

change from happening and cannot, therefore, characterize the main type of instability that leads to change in community structure. The assumption of May (1972) that variations in the strength of intraspecific competition are unimportant is one that has been largely neglected (see, however, de Angelis 1975; Haydon 1994, 2000; de Ruiter et al. 1995; Neutel et al. 2002). The effect of this assumption is at least as prominent as the assumptions concerning off-diagonal community elements.

Technical detail and exhaustive testing are unavoidable ingredients in the preceding analysis, but a clear and practical biological message emerges. Although there is a relationship between stability and complexity in ecological communities, the predictive power of this relationship is weak. Honest and seemingly pragmatic attempts to replace ignorance of ecological detail with random numbers, whether these relate to network structure or to interactions between species, must be treated with extreme caution. Despite the limitations explained here in the context of local stability, random matrix models may be useful in the context of more general coexistence conditions, where they can lead to quantitative predictions of community structure in good agreement with observations (Meszéna et al. 2006; Rossberg 2013).

On a further constructive note, we argue that using explicit dynamic models to describe ecological networks is preferable to directly assigning elements to a community matrix without reference to the underlying population dynamics. Parameterizing a dynamic model requires additional data—for example, species' intrinsic growth rates or equilibrium biomass densities—as well as estimates of interaction strengths. Collecting these data is not always practical. Nevertheless, estimating them by means of established models (de Ruiter et al. 1995; Emmerson and Raffaelli 2004; Datta et al. 2010) or investigating the effects of introducing variability in them is preferable to simply assuming that they satisfy an arbitrary set of mathematical constraints.

#### Acknowledgments

We thank C. Hughes and L. Pastur for mathematical context and precision; S. Collings, R. Law, and A.-M. Neutel for discussions and comments; S. Allesina for critical input and for sharing preprints of his publication with us; and S. Diehl for insightful reviews. A.G.R. and J.B. were supported by the UK Department of Environment, Food and Rural Affairs (M1228) and by the European Commission (agreement 308392, DEVOTES).

#### Literature Cited

- Allesina, S., and M. Pascual. 2008. Network structure, predator-prey modules, and stability in large food webs. *Theoretical Ecology* 1:55–64.

- Allesina, S., and S. Tang. 2012. Stability criteria for complex ecosystems. *Nature* 483:205–208.
- Bastolla, U., M. A. Fortuna, A. Pascual-Garca, A. Ferrera, B. Luque, and J. Bascompte. 2009. The architecture of mutualistic networks minimizes competition and increases biodiversity. *Nature* 458: 1018–1020.
- Berlow, E. L., S. A. Navarrete, C. J. Briggs, M. E. Power, and B. A. Menge. 1999. Quantifying variation in the strengths of species interactions. *Ecology* 80:2206–2224.
- Brose, U., R. J. Williams, and N. D. Martinez. 2006. Allometric scaling enhances stability in complex food webs. *Ecology Letters* 9: 1228–1236.
- Christensen, V., and D. Pauly. 1992. Ecopath II—a software for balancing steady-state ecosystem models and calculating network characteristics. *Ecological Modelling* 61:169–185.
- Dalsgaard, J., S. S. Wallace, S. Salas, and D. Preikshot. 1998. Mass-balance model reconstructions of the Strait of Georgia: the present, one hundred, and five hundred years ago. Pages 72–91 in D. Pauly, T. Pitcher, D. Preikshot, and J. Hearne, eds. *Back to the future: reconstructing the Strait of Georgia ecosystem*. Vol. 6. Fisheries Centre Research Reports. University of British Columbia, Vancouver.
- Dambacher, J. M., H.-K. Luh, H. W. Li, and P. A. Rossignol. 2003. Qualitative stability and ambiguity in model ecosystems. *American Naturalist* 161:876–888.
- Datta, S., G. W. Delius, and R. Law. 2010. A jump-growth model for predator-prey dynamics: derivation and application to marine ecosystems. *Bulletin of Mathematical Biology* 72:1361–1382.
- de Angelis, D. L. 1975. Stability and connectance in food web models. *Ecology* 56:238–243.
- de Ruiter, P. C., A.-M. Neutel, and J. C. Moore. 1995. Energetics, patterns of interaction strengths, and stability in real ecosystems. *Science* 269:1257–1260.
- de Ruiter, P. C., J. A. Van Veen, J. C. Moore, L. Brussaard, and H. W. Hunt. 1993. Calculation of nitrogen mineralization in soil food webs. *Plant and Soil* 157:263–273.
- Elton, C. S. 1958. *The ecology of invasions by animals and plants*. Methuen, London.
- Emmerson, M. C., and D. Raffaelli. 2004. Predator-prey body size, interaction strength and the stability of a real food web. *Journal of Animal Ecology* 73:399–409.
- Emmerson, M. C., and J. M. Yearsley. 2004. Weak interactions, omnivory and emergent food-web properties. *Proceedings of the Royal Society B: Biological Sciences* 271:397–405.
- Erdős, P., and A. Rényi. 1960. On the evolution of random graphs. *Publications of the Mathematical Institute of the Hungarian Academy of Sciences* 5:17–61.
- Gravel, D., E. Canard, F. Guichard, and N. Mouquet. 2011. Persistence increases with diversity and connectance in trophic metacommunities. *PLoS ONE* 6:e19374. doi:10.1371/journal.pone.0019374.
- Gribble, N. A. 2005. Ecosystem modelling of the great barrier reef: a balanced trophic biomass approach. Pages 2561–2567 in A. Zenger and R. M. Argent, eds. *Modelling and Simulation Society of Australia and New Zealand*.
- Grimm, V., and C. Wissel. 1997. Babel, or the ecological stability discussions: an inventory and analysis of terminology and a guide for avoiding confusion. *Oecologia (Berlin)* 109:323–334.
- Guénette, S., and V. Christensen. 2005. Food web models and data for studying fisheries and environmental impacts on eastern Pacific ecosystems. Vol. 13. Fisheries Centre Research Reports. University of British Columbia, Vancouver.
- Haydon, D. 1994. Pivotal assumptions determining the relationship between stability and complexity: an analytical synthesis of the stability-complexity debate. *American Naturalist* 144:14–29.
- . 2000. Maximally stable model ecosystems can be highly connected. *Ecology* 81:2631–2636.
- Hofbauer, J., and K. Sigmund. 1998. *Evolutionary games and population dynamics*. Cambridge University Press, Cambridge.
- Jacquet, C., C. Moritz, L. Morissette, P. Legagneux, F. Massol, P. Archambault, and D. Gravel. 2013. No complexity-stability relationship in natural communities. arXiv preprint. arXiv:1307.5364.
- Jansen, W. 1987. A permanence theorem for replicator and Lotka-Volterra systems. *Journal of Mathematical Biology* 25:411–422.
- Jonsson, T., J. E. Cohen, and S. R. Carpenter. 2005. Food webs, body size, and species abundance in ecological community description. *Advances in Ecological Research* 36:1–84.
- Law, R., and J. C. Blackford. 1992. Self-assembling food webs: a global viewpoint of coexistence of species in Lotka-Volterra communities. *Ecology* 73:567–578.
- Levins, R. 1979. Coexistence in a variable environment. *American Naturalist* 114:765–783.
- MacArthur, R. 1955. Fluctuations of animal populations and a measure of community stability. *Ecology* 36:533–536.
- Mackinson, S., and G. Daskalov. 2007. An ecosystem model of the North Sea to support an ecosystem approach to fisheries management: description and parameterisation. *Cefas Science Series Technical Report* 142.
- May, R. M. 1972. Will a large complex system be stable? *Nature* 238:413–414.
- McCann, K., A. Hastings, and G. R. Huxel. 1998. Weak trophic interactions and the balance of nature. *Nature* 395:794–798.
- McCann, K. S. 2000. The diversity-stability debate. *Nature* 405:228–233.
- Meszéna, G., M. Gyllenberg, L. Pásztor, and J. A. J. Metz. 2006. Competitive exclusion and limiting similarity: a unified theory. *Theoretical Population Biology* 69:68–87.
- Metha, M. L. 1967. *Random matrices and the statistical theory of energy levels*. Academic Press, New York.
- Moellmann, C., and R. Diekmann. 2012. Marine ecosystem regime shifts induced by climate and overfishing: a review for the Northern Hemisphere. *Advances in Ecological Research* 47:303–347.
- Moore, J. C., P. C. de Ruiter, and H. W. Hunt. 1993. Influence of productivity on the stability of real and model ecosystems. *Science* 261:906–908.
- Moore, J. C., P. C. de Ruiter, H. W. Hunt, D. C. Coleman, and D. W. Freckman. 1996. Microcosms and soil ecology: critical linkages between field studies and modelling food webs. *Ecology* 77:694–705.
- Neutel, A.-M., J. A. P. Heesterbeek, and P. C. de Ruiter. 2002. Stability in real food webs: weak links in long loops. *Science* 296:1120–1123.
- Neutel, A.-M., J. A. P. Heesterbeek, J. van de Koppel, G. Hoenderboom, A. Vos, C. Kaldeway, F. Berendse, and P. C. de Ruiter. 2007. Reconciling complexity with stability in naturally assembling food webs. *Nature* 449:599–602.
- O’Gorman, E. J., and M. C. Emmerson. 2010. Manipulating interaction strengths and the consequences for trivariate patterns in a marine food web. *Advances in Ecological Research* 42:301–419.
- Opitz, S. 1996. Trophic interactions in Caribbean coral reefs. *Technical Report* 43. International Center for Living Aquatic Resources Management, Makati.

- Otto, S. B., B. C. Rall, and U. Brose. 2007. Allometric degree distributions facilitate food-web stability. *Nature* 450:1226–1229.
- Pawar, S., A. I. Dell, and V. M. Savage. 2012. Dimensionality of consumer search space drives trophic interaction strengths. *Nature* 486:485–489.
- Pimm, S. L. 1980. Food web design and the effect of species deletion. *Oikos* 35:139–149.
- Pimm, S. L., and J. H. Lawton. 1978. On feeding on more than one trophic level. *Nature* 275:542–544.
- Reuman, D. C., C. Mulder, C. Banašek-Richter, M.-F. Cattin Blandenier, A. M. Breure, H. D. Hollander, J. M. Kneitel, D. Raffaelli, G. Woodward, and J. E. Cohen. 2009. Allometry of body size and abundance in 166 food webs. *Advances in Ecological Research* 41:1–44.
- Rossberg, A. G. 2013. *Food webs and biodiversity: foundations, models, data*. Wiley, Hoboken, NJ.
- Staniczenko, P. P. A., J. C. Kopp, and S. Allesina. 2013. The ghost of nestedness in ecological networks. *Nature Communications* 4:1391.
- Tang, S., S. Pawar, and S. Allesina. 2014. Correlation between interaction strengths drives stability in large ecological networks. *Ecology Letters* 17:1094–1100.
- Thébault, E., and C. Fontaine. 2010. Stability of ecological communities and the architecture of mutualistic and trophic networks. *Science* 329:853–856.
- Twomey, M., U. Jacob, and M. C. Emmerson. 2012. Perturbing a marine food web: consequences for food web structure and tri-variate patterns. *Advances in Ecological Research* 47:349–409.
- Tylianakis, J. M., E. Laliberté, A. Nielsen, and J. Bascompte. 2010. Conservation of species interaction networks. *Biological Conservation* 143:2270–2279.
- Walters, C., S. J. D. Martell, and B. Mahmoudi. 2006. An Eco-sim model for exploring ecosystem management options for the Gulf of Mexico: implications of including multistanza life history models for policy predictions. Presentation for Mote Symposium 6:23.
- Wiggins, S. 2003. *Introduction to applied nonlinear dynamical systems and chaos*. Vol. 2. Springer, New York.
- Woodward, G., B. Ebenman, M. Emmerson, J. M. Montoya, J. M. Olesen, A. Valido, and P. H. Warren. 2005a. Body size in ecological networks. *Trends in Ecology and Evolution* 20:402–409.
- Woodward, G., D. C. Speirs, and A. G. Hildrew. 2005b. Quantification and resolution of a complex, size-structured food web. *Advances in Ecological Research* 36:85–135.
- Yodzis, P. 1981. The stability of real ecosystems. *Nature* 289:674–676.

Associate Editor: Michael G. Neubert  
Editor: Troy Day



“Of that class of the feathered creation to which the term Birds of Paradise has been applied, and which they certainly most appropriately bear, New Guinea with its adjacent islands is the home. . . . These favored regions, besides those of the Aru Islands, where birds of paradise also abound, are rich in vegetation beyond even the usual fecundity of the tropics. Almost as unique, varied and lovely, are other forms of animal life—butterflies, dragon-flies, lizards, insects great and small, and countless tribes of the feathered race.” From “Some Birds of Paradise from New Guinea” by Geo. S. Mead (*The American Naturalist*, 1894, 28:915–920).

# Appendix A from A. James et al., “Constructing Random Matrices to Represent Real Ecosystems” (Am. Nat., vol. 185, no. 5, p. 000)

## Empirically Derived Community Matrices

The 21 empirically derived community matrices are available in electronic form. This section describes the methods used to obtain these data for each class of food web studied.

### *Biomass Flux Method*

Eight successional soil food webs and four soil food webs were supplied by Anje-Margriet Neutel from the data published in de Ruiter et al. (1993, 1995), Moore et al. (1993, 1996), and Neutel et al. (2002). The elements of the community matrix were derived from a generalized Lotka-Volterra-type model of the same form as equation (5) at equilibrium. For primary producers,  $r_i > 0$  was the intrinsic rate of increase per year. For consumers,  $r_i < 0$  was the nonpredatory death rate per year. For a species  $i$  that is consumed by species  $j$ , the Lotka-Volterra coefficient  $q_{ij}$  was set equal to the negative of the consumption coefficient (in units of  $\text{g}^{-1} \text{m}^2 \text{yr}^{-1}$ )  $c_{ij}$ ; the Lotka-Volterra coefficient  $q_{ji}$  was set equal to the assimilation efficiency of species  $j$  times the production efficiency of species  $j$  times the consumption coefficient  $c_{ij}$ . Species were aggregated into functional groups of species with similar food sources. Intrinsic birth and death rates and efficiencies were estimated from microcosm studies. Trophic interactions among taxa were established by direct observation or gut content analysis (Moore et al. 1996). Consumption coefficients were estimated from the measured biomass flux from prey to predator (Moore et al. 1993). The original data included a row and a column corresponding to detritus; these were removed for this analysis.

In the eight successional food webs, the average number of species was 12 (range, 7–15), mean connectance was 0.29 (range, 0.28–0.34), and average pairwise correlation  $\rho$  (i.e., correlation between  $a_{ij}$  and  $a_{ji}$ ) was  $-0.062$  (range,  $-0.02$  to  $-0.13$ ). In the four soil food webs, the average number of species was 17 (range, 16–18), mean connectance was 0.27 (range, 0.23–0.31) and average pairwise correlation was  $-0.055$  (range,  $-0.047$  to  $-0.059$ ). All of the networks were strictly predator-prey (i.e.,  $a_{ij}$  and  $a_{ji}$  either had opposite signs or were both 0).

### *Predator-Prey Mass Ratio Method*

Data were obtained for the average adult body mass  $w_i$  of species  $i$  and which species predated on which other species for the well-documented Ythan Estuary (Emmerson and Raffaelli 2004), Broadstone Stream (Woodward et al. 2005b), and Tuesday Lake 1984 (Jonsson et al. 2005) food webs. In the case of Tuesday Lake, 56 species were aggregated into 21 functional groups with identical links (trophic species). We used the average body mass of all species in a functional group as the body mass for that trophic species. Species with no observed predator or prey links were discarded.

The model of Emmerson and Raffaelli (2004) was used to estimate elements of the community matrix for both of these food webs. For each predator-prey pair, the Lotka-Volterra coefficient  $q_{ij}$  was assumed to be a power law function of the ratio of predator body size  $w_j$  to prey body size  $w_i$ :

$$q_{ij} = -q_0 \left( \frac{w_j}{w_i} \right)^{q_1}. \quad (\text{A1})$$

The corresponding element  $q_{ji}$  is opposite in sign and reduced in magnitude by a factor  $\epsilon_j$ , representing the predator's feeding efficiency:  $q_{ji} = -\epsilon_j q_{ij}$ . The equilibrium biomass  $x_i^*$  of species  $i$  was estimated to be

$$x_i^* = x_0 w_i^{q_2}. \quad (\text{A2})$$

The community matrix elements were then calculated via  $a_{ij} = q_{ij} x_i^*$ . Parameter values were  $q_0 = 7 \times 10^{-4}$ ,  $x_0 = 95.92$ ,  $q_1 = 0.66$ , and  $q_2 = -0.1836$ . A fixed efficiency of  $\epsilon = 0.1$  was used for all species.

The average number of species in these webs was 47 (range, 21–88), mean connectance was 0.24 (range, 0.11–0.32), and average pairwise correlation  $\rho$  was  $-0.75$  (range,  $-0.28$  to  $-0.98$ ).

### *Ecopath with Ecosim (EwE)*

The Ecosim community matrices were constructed in two steps. First, an Ecopath (Christensen and Pauly 1992) model was set up, representing a balanced account of biomass flows through the ecosystem constrained by empirical data on abundances, metabolic rates, and feeding preferences. From such a static Ecopath model, a dynamic Ecosim model was derived by modeling energy flows as outcomes of population-dynamic processes (feeding, respiration, mortality). This led to expressions for  $\mathbf{f}(\mathbf{x})$ , from which the community matrix can be computed. The time derivatives  $\mathbf{f}(\mathbf{x})$  were given by the derivt function of Ecosim. Numerically differentiating the output of this function with respect to the biomass  $x_j$  of species  $j$  gives the  $j$ th column of the community matrix.

The six marine food webs were (1) the Tampa Bay model, which is a subset consisting of 52 groups of the Gulf of Mexico model (Walters et al. 2006); (2) the Georgia Strait (British Columbia) model (Dalsgaard et al. 1998), a model consisting of 27 functional groups; (3) the Caribbean Reef model (50 groups; Opitz 1996); (4) the Northeast Pacific model (40 groups; Gu nette and Christensen 2005); (5) the Great Barrier Reef model (32 groups; Gribble 2005); and (6) the Centre for Environment, Fisheries and Aquaculture Science (Cefas) North Sea model (70 groups; Mackinson and Daskalov 2007). The EwE models for data sets 1–5 can be downloaded from the University of British Columbia website (<http://sources.ecopath.org>; password required for 1 and 2 and may be found at <http://www.ecopath.org/models> for 3–5). The model for data set 6 is available by contacting one of the Cefas authors.

All of these food webs contain a substantial number of nonpredator-prey interactions, where either  $a_{ij}$  and  $a_{ji}$  have the same sign or one of  $a_{ij}$  and  $a_{ji}$  is 0 and the other is not 0. The Tampa Bay and North Sea models contain multistanza (i.e., age-structured) groups for the same species. Each stanza is a separate node and a part of the population of stanza  $m$  of species  $n$  flows into stanza  $m + 1$  of species  $n$ , creating a  $(+, 0)$  type link. Thus, it is not possible to order the species so that all elements in the lower matrix triangle are positive and all elements in the upper matrix triangle are negative. We therefore designed the randomization algorithms (see below) so that they can be applied to any community matrix, regardless of sign structure.

The average number of species in these webs was 45 (range, 27–70), mean connectance was 0.56 (range, 0.34–0.70), and average pairwise correlation  $\rho$  was  $-0.057$  (range,  $-0.0097$  to  $-0.28$ ).

### *Stability Criteria*

The values of  $d_0$  in the stability criteria of equations (3) and (4) were calculated for each empirically derived community matrix. In these equations,  $S$  is the number of species in the matrix;  $C$  is the connectance (i.e., the number of links divided by  $S(S - 1)$ );  $\sigma$  is the standard deviation of the nonzero off-diagonal matrix elements;  $E$  and  $V$  are the mean and variance, respectively, of all off-diagonal elements; and  $\rho$  is the pairwise correlation (Tang et al. 2014):

$$\rho = \frac{E(a_{ij}a_{ji}) - E^2}{V}. \quad (\text{A3})$$

The stability criterion in equation (3) is valid only for matrices where  $(SV)^{1/2}(1 + \rho) > SE$  (Tang et al. 2014). This was checked and found to be true for all of our empirically derived community matrices.



## Appendix B from A. James et al., “Constructing Random Matrices to Represent Real Ecosystems” (Am. Nat., vol. 185, no. 5, p. 000)

### Randomization Algorithms

These algorithms randomize an  $S \times S$  matrix  $A = [a_{ij}]$  to create an  $S \times S$  matrix  $B = [b_{ij}]$ .  $N_1$  is the number of nonzero off-diagonal elements, and  $C = N_1/[S(S - 1)]$  is the fraction of off-diagonal elements that are nonzero. The mean and standard deviation of the nonzero elements are  $\mu$  and  $\sigma$ , respectively. The mean of the positive and negative elements are  $\mu_+$  and  $\mu_-$ . The number of elements involved in a cycle of length three is  $N_c$  (in cases where links are not bidirectional—i.e., only one of  $a_{ij}$  and  $a_{ji}$  is nonzero—an element is considered to be in a cycle regardless of the signs of the element); the number of nonzero elements not involved in a cycle of length three is  $N_0 = N_1 - N_c$ .

#### Off-Diagonal Algorithms

All of the off-diagonal algorithms hold the diagonal elements 0. Any randomization that resulted in a species having no interactions (i.e., every entry in a row or column was 0) or that contained no cycles was rejected, as these randomizations have a 0 leading eigenvalue. Algorithms used in figures 2 and 3 are as follows:

- A. *Random topology; randomly generated entries.* Each randomization has  $N_1$  entries sampled from a normal distribution  $N(0, \sigma^2)$ . Entries are positioned randomly.
- B. *Random topology with sign structure; randomly generated entries.* Each randomization has  $N_1$  randomly positioned entries. Positive (negative) entries are sampled from the half-normal distribution with mean  $\mu_+$  ( $\mu_-$ ). For every element pair  $(a_{ij}, a_{ji})$  (with  $i < j$ ) in the empirically derived matrix with a particular sign structure—that is,  $(+, +)$ ,  $(+, -)$ ,  $(-, 0)$ , and so on—there is a random pair  $(b_{kl}, b_{lk})$  (with  $k < l$ ) with the same sign structure.
- C. *Empirical topology; randomly generated entries.* An element  $b_{ij}$  is nonzero if and only if the corresponding element in the empirically derived matrix,  $a_{ij}$ , is nonzero. Furthermore,  $\text{sign}(a_{ij}) = \text{sign}(b_{ij})$ . Positive (negative) entries are sampled from the half-normal distribution with mean  $\mu_+$  ( $\mu_-$ ).
- D. *Random topology; randomly generated entries preserving row structure.* Each randomization has  $N_1$  entries placed at random. The randomized matrix contains the same proportion of each pair type  $((+, +)$ ,  $(-, 0)$ ,  $(+, -)$ , etc.) as the original matrix. The mean of the positive (negative) entries of row  $i$  of the empirically derived matrix is  $\mu_{i+}$  ( $\mu_{i-}$ ). Where there are no entries of that sign in a row, the value of  $\mu_{i\pm}$  from a populated row (chosen at random) is used instead. Positive (negative) entries in row  $i$  of the randomized matrix are sampled from a normal distribution with mean  $\mu_{i+}$  ( $\mu_{i-}$ ) and coefficient of variation 0.2.
- E. *Random topology; empirical entries (paired).* Each element  $a_{ij}$ , where  $i < j$ , is moved to element  $b_{kl}$ , where  $k < l$ . For every move of  $a_{ij}$  to  $b_{kl}$ , there is a corresponding move of  $a_{ji}$  to  $b_{lk}$ , preserving the pair structure of the empirically derived matrix.
- F. *Empirical topology; empirical entries (paired).* Each element pair  $(a_{ij}, a_{ji})$ , where  $i < j$ , is swapped with an element pair  $(a_{kl}, a_{lk})$ , where  $k < l$ , that has the same sign structure, that is,  $(+, +)$ ,  $(-, +)$ ,  $(0, -)$ , and so on.
- G. *Empirical topology; empirical entries (not paired).* Every positive element is swapped with another positive element. Every negative element is swapped with another negative element.
- H. *Random topology; empirical entries (constrained within rows/columns).* This algorithm permutes elements of the empirically derived matrix within rows while preserving  $(a_{ij}, a_{ji})$  pairs. Most of the empirically derived community matrices are organized with top predators in the upper rows and basal resources in the lower rows. This tends to lead a triangular structure in the matrix, where the lower-left triangle contains predominantly negative elements and the upper-right triangle contains predominantly positive elements. This means that the lower triangle typically contains elements that have, on average, a larger magnitude than the elements in the upper triangle. The row structure of the empirically derived matrices therefore tends to be stronger in the lower

triangle, so we designed the algorithm described above to preserve row structure in the lower triangle (and therefore column structure in the upper triangle).

Each nonzero lower triangle element  $a_{ij}$  (where  $i > j$ ) is moved within the same row to  $b_{ik}$  (where  $i > k$ ). To preserve the pair structure of the original matrix, this move of  $a_{ij}$  to  $a_{ik}$  is accompanied by a corresponding move of  $a_{ji}$  to  $b_{ki}$ .

We also tested a similar algorithm that preserved row structure in the upper triangle and column structure in the lower triangle; this produced matrices with leading eigenvalues farther away from the leading eigenvalue of the empirically derived matrix.

The randomization algorithms for figure 4 are as follows:

- A (vertical axis). *Random topology holding cycles of length three; empirical entries (paired)*. This is a constrained version of randomization D from figures 2 and 3. The  $N_c$  elements that are part of a cycle of length three are fixed (i.e., their position was not changed). The remaining  $N_0$  elements are moved as described in D above.
- A (horizontal axis). *Random topology holding some entries; empirical entries (paired)*. This is a constrained version of randomization D from figures 2 and 3.  $N_c$  elements are chosen at random. These elements are fixed. The remaining  $N_0$  elements are moved as described in D above.
- B (vertical axis). *Empirical topology holding cycles of length three; empirical entries (paired)*. This is a constrained version of randomization E from figures 2 and 3. The  $N_c$  elements that are part of a cycle of length three are fixed. The remaining  $N_0$  elements are swapped as described in E above.
- B (horizontal axis). *Empirical topology holding some entries; empirical entries (paired)*. This is a constrained version of randomization E from figures 2 and 3.  $N_c$  elements are chosen at random. These elements are fixed. The remaining  $N_0$  elements are swapped as described in E above.

Table B1 gives a summary of the properties preserved by each algorithm and measures of the bias in  $d$ .

### Diagonal Algorithm

In figure 5A, the diagonal elements were replaced with normally distributed random numbers with mean 0 and variance  $\sigma^2$ , that is, the variance of the nonzero off-diagonal elements.

**Table B1:** Properties preserved by each off-diagonal randomization algorithm

Figure	Pairs	Elements	Topology	Cycles	Rows	Limited changes	E(error)	P(under)
2A	×	×	×	×	×	×	2.29	.03
2B	✓	×	×	×	×	×	1.7	.14
2C	✓	✓	✓	×	×	×	1.24	.14
2D	×	×	×	×	✓	×	.24 <sup>a</sup>	.42 <sup>a</sup>
2E	✓	✓	×	×	×	×	1.21	.13
2F	✓	✓	✓	×	×	×	1.01	.16
2G	✓	✓	×	×	×	×	1.31	.12
2H	✓	✓	×	×	✓	×	.49	.29
4A (y)	✓	✓	×	✓	×	✓	.70	.09
4A (x)	✓	✓	×	×	×	✓	.77	.05
4B (y)	✓	✓	✓	✓	×	✓	.24	.21
4B (x)	✓	✓	✓	×	×	✓	.67	.08

Note: Pairs:  $b_{ij} \neq 0$  if and only if  $b_{ji} \neq 0$ . Elements: the elements of the original matrix were permuted rather than using random deviates from a probability distribution. Topology: the original network topology was preserved. Cycles: the positions and weights of the cycles of length three was preserved. Rows: the row structure was preserved. Limited changes: the number of elements of the original matrix that were moved was limited to be the same as in the corresponding cycle-preserving algorithm. E(error) is the mean value of error =  $\log_{10}(I_{\text{rand}}/I_{\text{emp}})$  of 200 realizations of the randomization scheme across the 21 empirically derived matrices. P(under) is the proportion of realizations for which the error is negative. An unbiased randomization scheme would have E(error) = 0 and P(under) = 0.5.

<sup>a</sup> Do not include freshwater webs, as this algorithm does not preserve pairwise structure and as expected gives very poor results for these matrices.

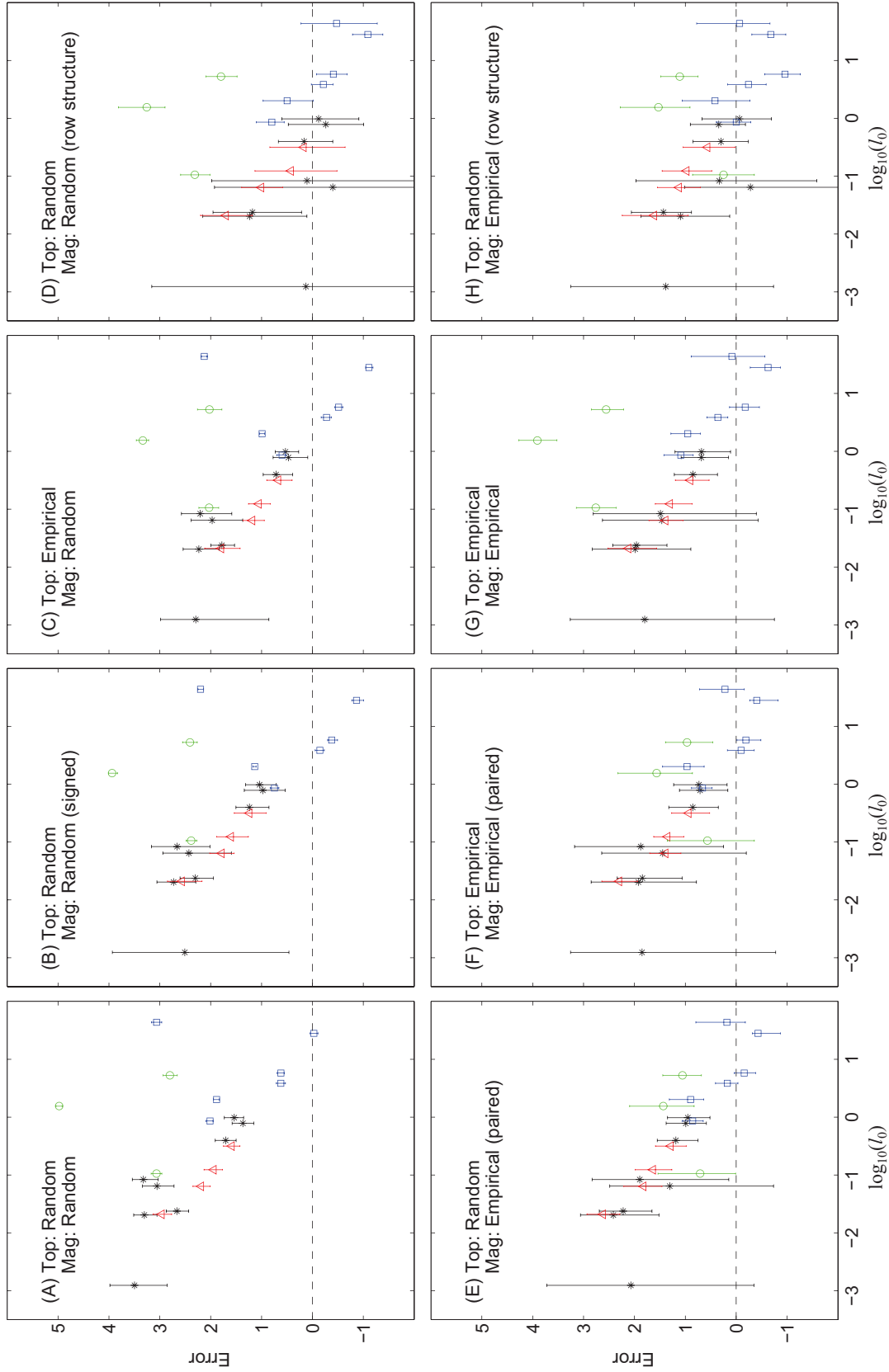


**Figure B1:** Figure 3 redrawn with the matrices ordered by  $l_0$ , the real part of the leading eigenvalue of the empirically derived matrix, for the same six randomization algorithms (A–F) as in figure 3, changing either or both of network topology (Top) and magnitude of interaction strengths (Mag). Symbols indicate the method used to construct the community matrix: biomass flux = stars (successional webs) or triangles (soil webs); Ecopath with Ecosim = squares; predator-prey mass ratio = circles.

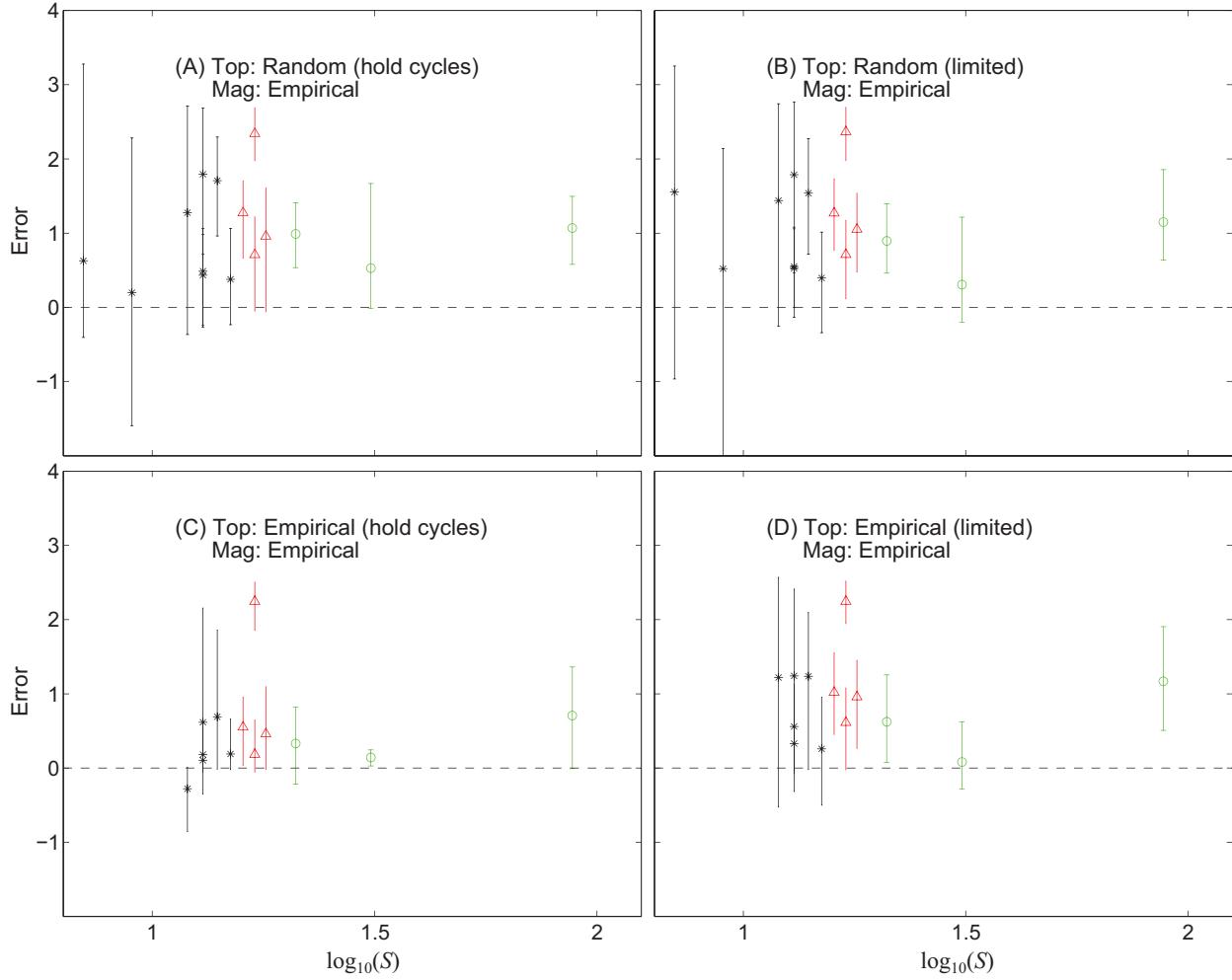


**Figure B2:** Distribution of error =  $\log_{10}(I_{\text{rand}}/I_{\text{emp}})$  for the four randomization algorithms used in figure 4. Figure 4A plots algorithm A against algorithm B; figure 4B plots algorithm C against algorithm D. The food webs are plotted against the number of species  $S$  in the web on the horizontal axis. Symbols indicate the method used to construct the community matrix: biomass flux = stars (successional webs) or triangles (soil webs); predator-prey mass ratio = circles. Community matrices for which <90% of randomizations produce distinct matrices are not shown; this includes all of the Ecopath with Ecosim webs.

## Appendix C from A. James et al., “Constructing Random Matrices to Represent Real Ecosystems” (Am. Nat., vol. 185, no. 5, p. 000)

### Dynamic Model Bifurcation Analysis

Consider the generalized Lotka-Volterra model

$$\frac{dx_i}{dt} = x_i \left( r_i + \sum_{j=1}^S q_{ij} x_j \right), \quad i = 1, \dots, S, \quad (C1)$$

where  $x_i$  is the biomass density of species  $i$ ,  $r_i$  is the intrinsic growth rate of species  $i$ , and  $q_{ij}$  are Lotka-Volterra coefficients. To prevent boundless growth of species  $i$  in isolation, the elements  $q_{ii}$  must not be positive. Equation (C1) has an equilibrium point  $\mathbf{x}^*$  satisfying  $Q\mathbf{x}^* = -\mathbf{r}$ . At this equilibrium, the diagonal elements of the community matrix are  $a_{ii} = q_{ii}x_i^*$ . If  $x_i^* > 0$  for all  $i$ , this equilibrium corresponds to the coexistence of all species. If, as the model parameters are varied,  $x_j^*$  becomes negative for some  $j$ , there is a transcritical bifurcation, and a different equilibrium, with  $x_j^* = 0$ , becomes stable. Hence, species  $j$  becomes extinct via a gradual decline of  $x_j^*$  to 0, and, at the transcritical bifurcation,  $a_{jj} = 0$ .

Now consider the effect of requiring the diagonal elements of the community matrix to be equal,  $a_{ii} = -d < 0$ . Combining this with the equilibrium condition  $Q\mathbf{x}^* = -\mathbf{r}$  shows that the intrinsic growth rates  $r_i$  must satisfy

$$r_i = d \sum_{j=1}^S \frac{q_{ij}}{q_{jj}}, \quad i = 1, \dots, S, \quad (C2)$$

which is equation (6) in the main text. This implies that basal species  $i$ , which are negatively influenced by their interactions with other species and so have  $q_{ij} < 0$ , will always have positive  $r_i$  (recall that  $q_{ij} < 0$ ). Top predators, which are positively influenced by their interactions and so have  $q_{ij} > 0$  ( $i \neq j$ ), will typically have negative  $r_i$ .

Under the constraint in equation (C2), the equilibrium equation  $Q\mathbf{x}^* + \mathbf{r} = 0$  becomes  $Q(\mathbf{x}^* - \mathbf{v}) = 0$ , where  $v_i = -d/q_{ii}$ , which is always positive since  $d > 0$  and  $q_{ii} < 0$ . Hence, there is always a positive equilibrium with  $x_i^* = v_i$ . This equilibrium cannot undergo a transcritical bifurcation with another equilibrium for which  $v_j^* = 0$  for some  $j$ . The only way a species can become extinct is if the matrix  $Q$  becomes rank deficient, which leads to a line of nonisolated equilibria through the point  $\mathbf{x}^* = \mathbf{v}$ . The positive equilibrium at  $\mathbf{x}^* = \mathbf{v}$  suddenly becomes unstable, and an equilibrium in which one or more species is 0 suddenly becomes stable.

Figure C1 illustrates the bifurcation structure of the model, with and without the constraint imposed by equation (C2), for the simple two-species case. In the constrained model (fig. C1A–C1C), the two nullclines are forced to intersect at the point  $(x_1, x_2) = (-d/q_{11}, -d/q_{22})$ . As  $q_{ij}$  are varied, the equilibrium must always remain in the interior of the positive quadrant because  $q_{ii}$  must be nonpositive and finite. Therefore, no transcritical bifurcations are possible. The only way in which a species can become extinct is if the nullclines become parallel (in the two-species model, this requires  $q_{12}$  and  $q_{21}$  to have the same sign). If this happens, the nullclines coincide and there is a line of nonisolated equilibria passing through  $(-d/q_{11}, -d/q_{22})$ . After this bifurcation, the equilibrium at  $(-d/q_{11}, -d/q_{22})$  loses stability, and one of the two species becomes extinct.

In the unconstrained model (fig. C1D–C1F), the slopes and intercepts of the nullclines can vary independently as model parameters are varied. The coexistence equilibrium point can therefore move outside the positive quadrant and lose stability via a transcritical bifurcation. For example, in the transition from figure C1D to C1E, species 2 gradually declines to 0, at which point there is a transcritical bifurcation. The coexistence equilibrium moves outside the feasible region, and the species 1 equilibrium  $(x_1, x_2) = (0, -r_2/q_{22})$  becomes stable.

In figure C1, we used a competition model ( $q_{12}, q_{21} < 0$ ) because, in the constrained two-species case, a bifurcation can occur only when  $q_{12}q_{21} = 1$ , which requires  $q_{12}$  and  $q_{21}$  to have the same sign. For models with more species, the scenario is not limited to competitive interactions: bifurcations occur in the constrained model when the matrix  $Q$  becomes rank deficient, which can happen in predator-prey models as well as competition models.

The result that constraining diagonal elements of the community matrix to be equal precludes transcritical bifurcations is not particular to the generalized Lotka-Volterra model in equation (C1). Consider a more general model where the rate of change of species  $i$  is

$$\frac{dx_i}{dt} = x_i(r_i + q_{ii}x_i + h_i(\mathbf{x})), \quad i = 1, \dots, S \quad (\text{C3})$$

for some function  $h_i(\mathbf{x})$ . If we require that ( $x_j = 0 \forall j \neq i \Rightarrow h_i(\mathbf{x}) = 0$ ), then, as for the generalized Lotka-Volterra model, each species, in isolation, behaves according to a logistic equation with intrinsic growth rate  $r_i$  (which can be positive or negative) and carrying capacity  $-r_i/q_{ii} > 0$ . However, the generalized Lotka-Volterra model assumes that  $h_i(\mathbf{x})$  is a linear function of  $x_i$ , whereas in equation (C3) the interaction terms contained in  $h_i(\mathbf{x})$  can be nonlinear, for example, representing a type 2 response. The diagonal elements of the Jacobian matrix are

$$a_{ii} = r_i + 2q_{ii}x_i + h_i(\mathbf{x}) + x_i \frac{\partial h_i}{\partial x_i}. \quad (\text{C4})$$

Using the equilibrium condition from setting equation (C3) equal to 0, we obtain the diagonal elements of the Jacobian matrix at equilibrium:

$$a_{ii} = x_i^* \left( q_{ii} + \frac{\partial h_i}{\partial x_i} \Big|_{\mathbf{x}=\mathbf{x}^*} \right). \quad (\text{C5})$$

This shows that if species  $i$  becomes extinct via a transcritical bifurcation ( $x_i^* = 0$ ), then its diagonal element in the community matrix ( $a_{ii}$ ) must also be 0 at the bifurcation point. If instead the diagonal elements  $a_{ii}$  are all constrained to equal  $-d$ , then the equilibrium satisfies

$$x_i^* = -\frac{d}{q_{ii} + (\partial h_i / \partial x_i)|_{\mathbf{x}=\mathbf{x}^*}}. \quad (\text{C6})$$

Unlike in the constrained generalized Lotka-Volterra model, there is not always a unique positive equilibrium. There may be zero, one, or more solutions to equation (C6), some of which may have  $x_i^* < 0$  for some species. There may be saddle-node bifurcations that change the number of equilibria, and there may be Hopf bifurcations that change the stability of equilibria. Nevertheless, equation (C6) shows that it is impossible for  $x_i^*$  to pass smoothly through 0 as a model parameter is varied. Hence, transcritical bifurcations are impossible.

In general, requiring the diagonal elements of the community matrix to be equal imposes  $S$  constraints (e.g., eq. [C2]) on the model parameters. This is equivalent to taking a codimension  $S$  slice through the full model parameter space. The full parameter space is dominated by transcritical bifurcations, whereas the constrained codimension  $S$  parameter space has no transcritical bifurcations. The constrained model is therefore a singular case. It does not give a representative picture of the ways in which equilibria can gain or lose stability.

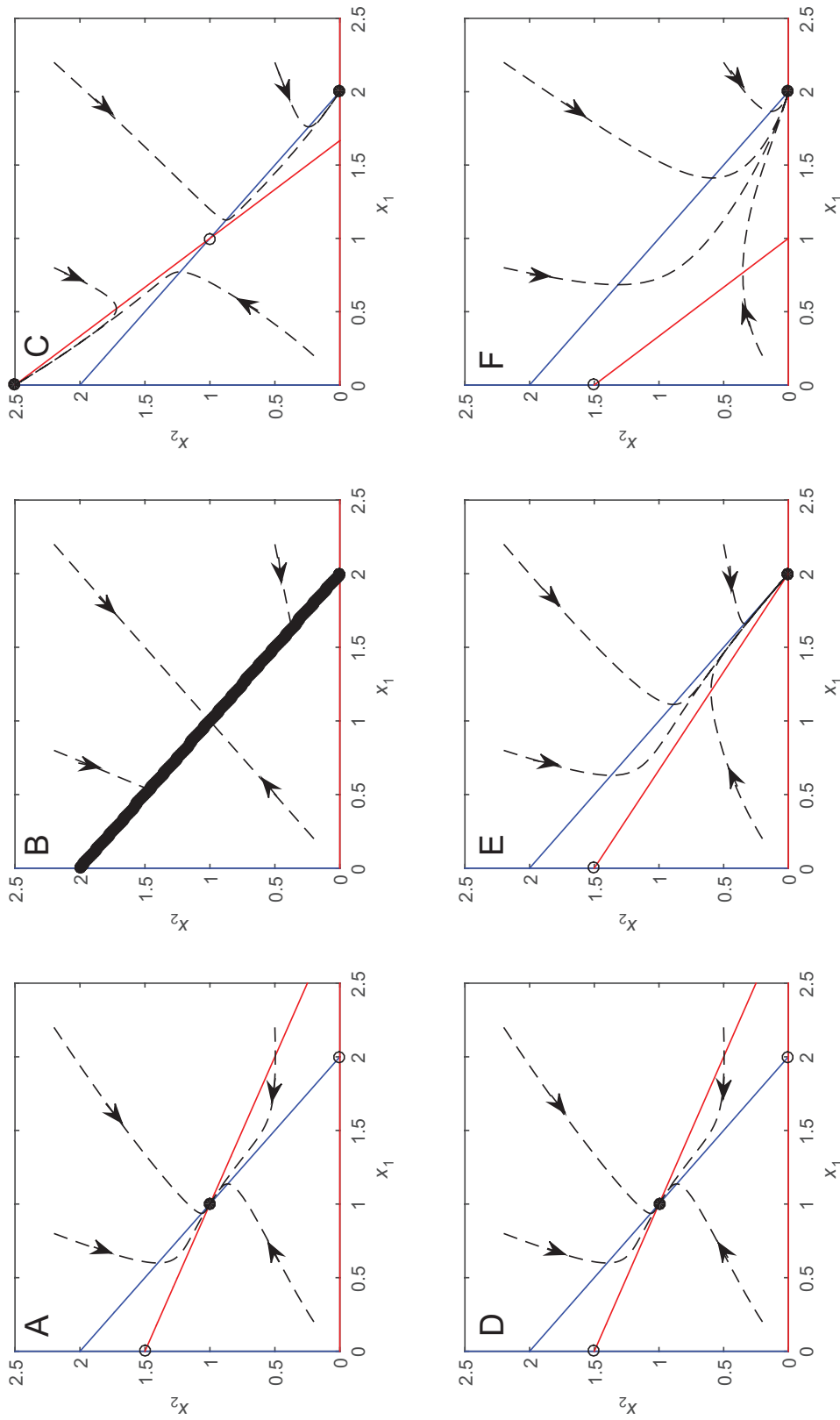


**Figure C1:** Phase planes for a two-species generalized Lotka-Volterra model (eq. [C1]). The blue lines are  $x_1$  nullclines, the red lines are  $x_2$  nullclines, the circles are equilibria (filled = stable; open = unstable), and the dashed curves are example orbits. A–C, Parameters are constrained by equation (C2): the nullclines are forced to cross at  $(x_1, x_2) = (-d/q_{11}, -d/q_{22})$ , which is always in the interior of the positive quadrant; at the bifurcation (B), the nullclines lie on top of one another, creating a line of nonisolated equilibria; after the bifurcation (C), one of the two species suddenly becomes extinct (which species depends on the initial condition). D–F, Parameters are not constrained: as the  $x_2$  nullcline steepens, the equilibrium density of species 2 gradually declines until the equilibrium collides with the single-species equilibrium on the axis, at which point a transcritical bifurcation occurs (E); after the bifurcation (F), species 2 is extinct. Parameter values:  $r_1 = 2, q_{11} = q_{22} = q_{12} = -1; A, q_{21} = -0.5, r_2 = 1.5; B, q_{21} = -1, r_2 = 2; C, q_{21} = -1.5, r_2 = 2.5; D, q_{21} = -0.5, r_2 = 1.5; E, q_{21} = -0.75, r_2 = 1.5; F, q_{21} = -1.5, r_2 = 1.5$ .